

Transverse-momentum-dependent semi-inclusive deep-inelastic scattering at HERMES

C. Van Hulse*,
on behalf of the HERMES Collaboration

University of the Basque Country - UPV/EHU

E-mail: cvhulse@mail.desy.de

Transverse-target-spin asymmetries as well as longitudinal beam-helicity asymmetries measured in semi-inclusive deep-inelastic scattering for charged pions and kaons and for protons and antiprotons are presented. They are extracted from data collected by the HERMES experiment using a 27.6 GeV longitudinally polarized electron and positron beam and, respectively, a transversely polarized hydrogen target and unpolarized hydrogen and deuterium targets. The measurements serve the determination of parton distribution functions describing the distribution of partons as a function of their longitudinal and transverse momenta in a transversely polarized proton as well as the quark-gluon-quark correlations inside the nucleon.

*XXIV International Workshop on Deep-Inelastic Scattering and Related Subjects
11-15 April, 2016
DESY Hamburg, Germany*

*Speaker.

1. Introduction

The nucleon structure can be described in terms of probability distributions of quarks and gluons as a function of the parton's longitudinal and transverse momenta, where longitudinal refers to the direction of the probe used to investigate the nucleon, or alternatively as a function of the parton's longitudinal momentum and transverse position. Different distributions exist depending on the considered spin state of the partons and nucleon. For the nucleon picture in terms of transverse position and longitudinal momentum, exclusive reactions provide the necessary information, while for the description in terms of longitudinal and transverse momenta, the study of semi-inclusive deep-inelastic scattering (DIS) as well as proton-proton collisions, complemented with the knowledge of fragmentation functions, themselves most easily accessible via electron-proton annihilation, procures the needed input.

In the here presented proceedings, the focus lies on the measurement of asymmetries extracted from semi-inclusive DIS, thus providing access to parton distributions as a function of longitudinal and transverse momenta. In particular, beam-helicity-dependent and beam-helicity-independent asymmetries extracted from data collected with a transversely polarized hydrogen target are discussed as well as the beam-helicity asymmetry extracted from semi-inclusive DIS measurements on unpolarized hydrogen and deuterium targets.

The distributions inside a transversely polarized proton are mapped out at leading twist in terms of transversely polarized quarks, by the transversity distribution, in terms of unpolarized quarks, by the Sivers distribution, in terms of again transversely polarized quarks but in addition probing the correlation with the quark transverse momentum, by the pretzelosity distribution, and finally in terms of longitudinally polarized quarks, by the worm-gear distribution. The transversity distribution survives integration over the transverse momentum of the quarks. The other three distributions do not survive integration over transverse momentum, but instead probe the correlation between the transverse momentum and the spin state. In order to access the worm-gear and pretzelosity distributions, a longitudinally polarized beam is needed, while the Sivers and transversity distributions are accessible using an unpolarized beam. Each of the distribution functions enters the semi-inclusive DIS cross section in pair with a fragmentation function. The Sivers and worm-gear distributions, both chiral-even, appear in combination with the spin-independent fragmentation function, which is chiral even, while the transversity and pretzelosity distributions, both chiral-odd, appear in combination with the Collins fragmentation function, itself also chiral odd. Apart from these distributions, specific higher-twist distributions, probing, e.g., quark-gluon-quark correlations, complete the picture for a transversely polarized nucleon. They are not discussed here.

The part of the cross section sensitive to the beam helicity and independent of the nucleon spin appears only at subleading twist. It is sensitive to quark-gluon-quark correlations and can at subleading twist be described in terms of combinations of leading-twist distribution functions (the spin-independent and Boer-Mulders distribution functions) and subleading-twist fragmentation functions (\tilde{G}^\perp and \tilde{E}) and combinations of subleading-twist distribution functions (e and g^\perp) and leading-twist fragmentation functions (the spin-independent and Collins fragmentation functions) [1].

Asymmetries are extracted from data collected by the HERMES experiment, formerly located in the east of the HERA storage ring at DESY in Hamburg. Here 27.6 GeV electrons and positrons

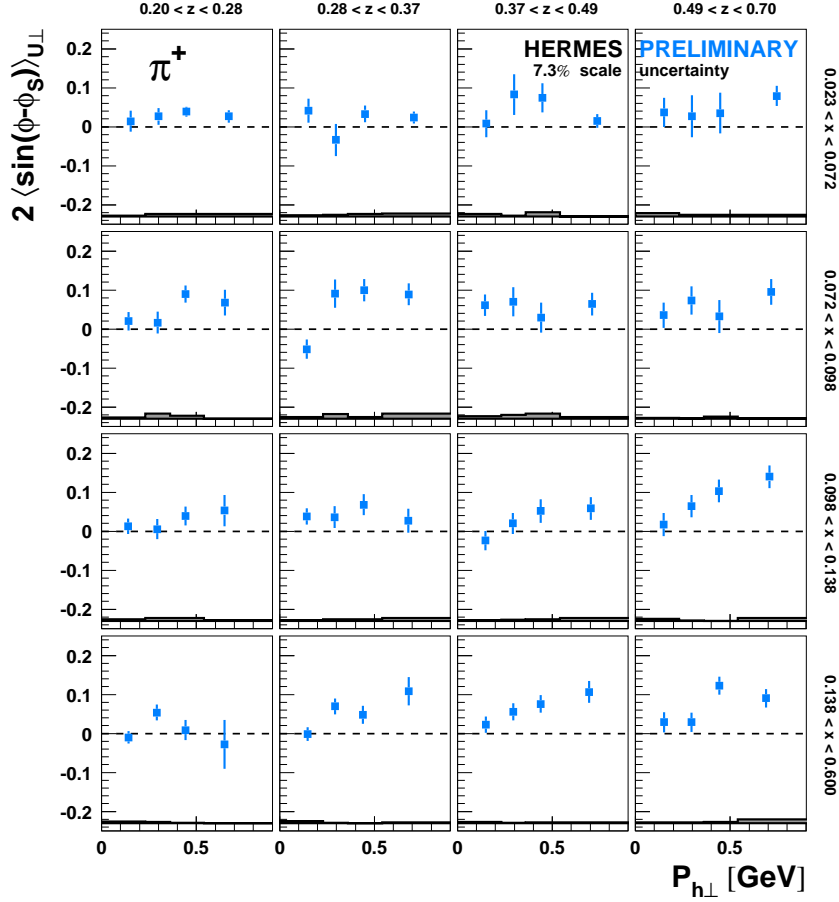


Figure 1: The Siverson amplitude for positive pions as a function of $P_{h\perp}$ for different bins in x (subdivision in rows) and z (subdivision in columns). The error bars (bands) indicate the statistical (systematic) uncertainty.

were scattered from various gaseous targets, internal to the beam, such as longitudinally and transversely polarized and unpolarized hydrogen, longitudinally polarized and unpolarized deuterium as well as heavier unpolarized targets.

The transverse-target-spin asymmetries are extracted for charged pions and kaons in three dimensions, simultaneously as a function of the Bjorken scaling variable x , the fractional hadron energy with respect to the virtual-photon energy z , and the transverse momentum of the hadron with respect to the virtual-photon momentum $P_{h\perp}$. These results extend earlier one-dimensional measurements by the HERMES experiment as a function of each of these kinematic variables of the Collins asymmetry, probing the transversity distribution and the Collins fragmentation function, the Siverson asymmetry, probing the Siverson distribution and the spin-independent fragmentation function [2–4], as well as the asymmetries sensitive to the pretzelosity and worm-gear distributions [5]. In addition, the same asymmetries for protons and for antiprotons are presented. While the extraction for protons is performed in one and three dimensions, limited statistical precision restricts the measurement for antiprotons to one dimension. For each of the hadron types, the asymmetries are

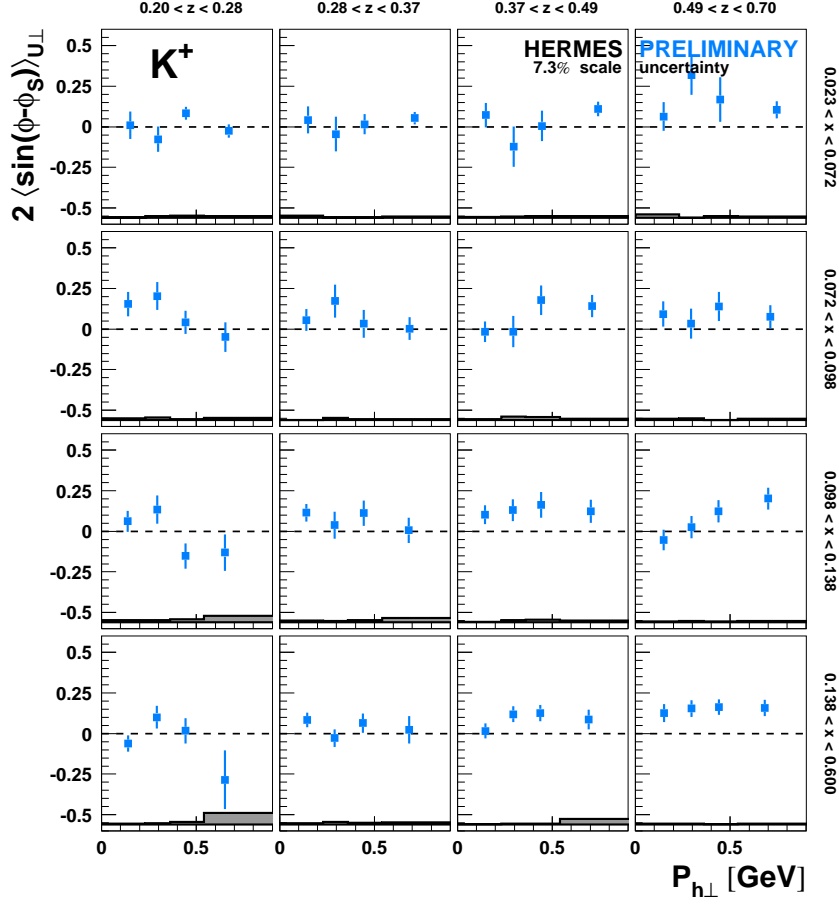


Figure 2: The Siverts amplitude for positive kaons as a function of $P_{h\perp}$ for different bins in x (subdivision in rows) and z (subdivision in columns). The error bars (bands) indicate the statistical (systematic) uncertainty.

simultaneously extracted from the collected data.

The subleading-twist beam-helicity asymmetry measured using unpolarized hydrogen and deuterium targets is also extracted in one and three dimensions for charged pions and kaons, and for protons and antiprotons, extending hereby the one-dimensional measurement for charged pions [6].

2. Transverse-target-spin asymmetries

The Siverts amplitudes for positive pions and kaons are shown in figures 1 and 2, respectively, as a function of $P_{h\perp}$ for different bins in x (rows) and z (columns). From the previous one-dimensional extraction by the HERMES collaboration, presented in Refs. [2,3], a rise of the Siverts amplitude with increasing $P_{h\perp}$ is observed for positive pions and kaons, while for their negatively charged counterparts, small asymmetries without outspoken kinematic dependencies are reported. From the here presented three-dimensional extraction, it is now seen that the rise of the amplitudes with increasing $P_{h\perp}$ is located at high values of x and z .

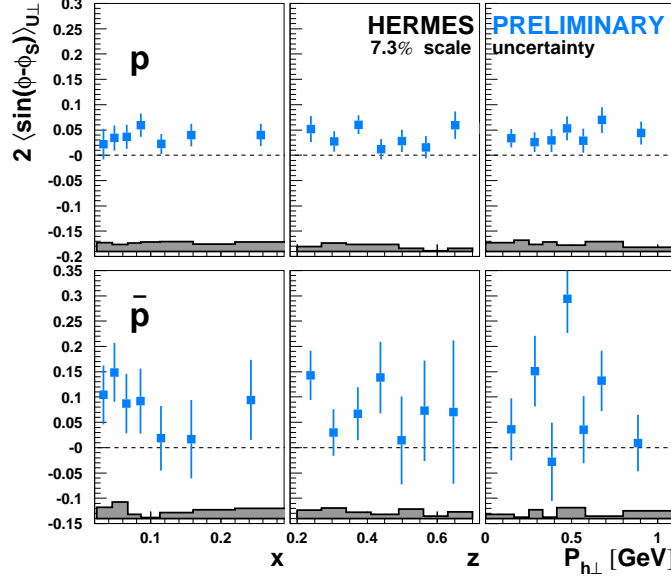


Figure 3: The Siverson amplitude for protons and antiprotons as a function of x (left panel), z (middle panel) and $P_{h\perp}$ (right panel). The error bars (bands) indicate the statistical (systematic) uncertainty.

In figure 3 the Siverson amplitudes for protons and antiprotons are presented in one dimension, as a function of x , z , and $P_{h\perp}$. The amplitude for protons is positive, without any outspoken kinematic dependence; the antiprotons exhibit an overall positive Siverson amplitude, but with substantial uncertainties. Also in the three-dimensional extraction, no outspoken kinematic dependencies are observed for protons.

The Collins amplitude for negative pions is shown in figure 4 as a function of x for different bins in z and $P_{h\perp}$. It is already reported in Refs. [2,4] that the Collins asymmetry for negative pions increases strongly in magnitude with increasing x . The three-dimensional extraction allows now to clarify that this increase of the amplitude with increasing x is concentrated at large values of $P_{h\perp}$, with a steeper increase with increasing z . For the other three mesons, the kinematic dependencies observed in one dimensions are not as clearly translated to the various phase-space regions in three dimensions. For protons and antiprotons, the latter exhibiting again large uncertainties, an overall negative, small Collins asymmetry without clear kinematic dependencies is observed.

In figure 5 the worm-gear amplitude for positive pions as a function of x for bins in z (rows) and $P_{h\perp}$ (columns) is presented. Earlier preliminary results in one dimension [5] show an overall positive amplitude, with a hint of a rise with increasing x for positive pions. In the three-dimensional extraction, no specific kinematic region can be isolated where this trend is observed. For negative pions and positive kaons small, positive amplitudes without explicit kinematic dependencies are observed, while for negative kaons, protons and antiprotons the amplitudes are compatible with

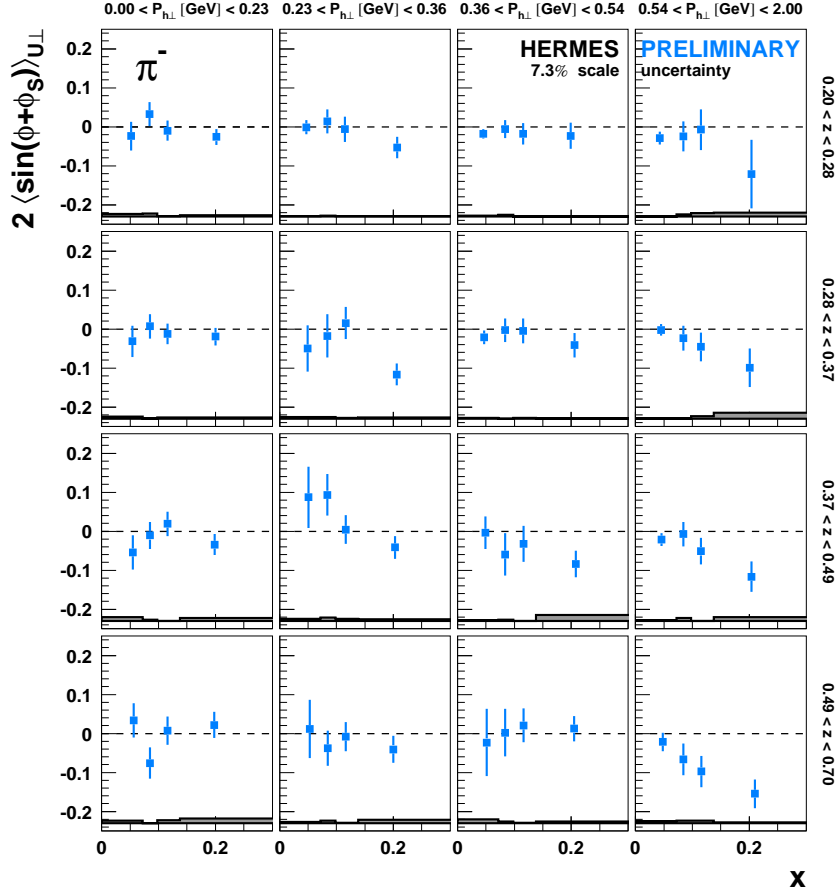


Figure 4: The Collins amplitude for negative pions as a function of x for different bins in z (subdivision in rows) and $P_{h\perp}$ (subdivision in columns). The error bars (bands) indicate the statistical (systematic) uncertainty.

zero.

The fourth and only remaining amplitude appearing at leading twist for scattering from a transversely polarized nucleon is the pretzelosity amplitude. It is not shown here. It is found to be small and without any explicit kinematic dependence for all here discussed hadrons.

3. Beam-helicity asymmetry

The beam-helicity asymmetry is shown in figure 6, top, for charged pions and kaons and in figure 6, bottom, for protons and antiprotons as a function of x , z , and $P_{h\perp}$ for data collected with a hydrogen target (filled circles) and with a deuterium target (open circles). The asymmetries for hydrogen and deuterium are compatible with each other. The asymmetry for positive pions is overall positive and rises with x and z , while there is a hint of a decrease as a function of $P_{h\perp}$. A similar dependency as a function of $P_{h\perp}$ is observed for negative pions. An analogous tendency can also not be excluded for kaons and protons. For negative pions, the rise as a function of z ,

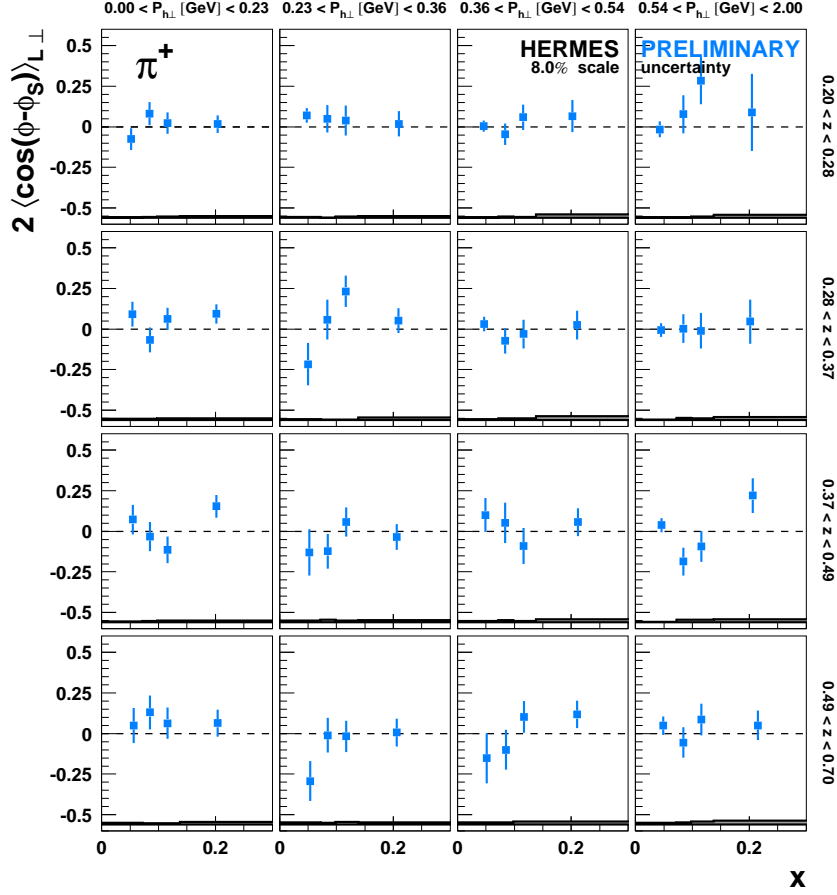


Figure 5: The Worm-gear amplitude for positive pions as a function of x for different bins in z (subdivision in rows) and $P_{h \perp}$ (subdivision in columns). The error bars (bands) indicate the statistical (systematic) uncertainty.

observed for positive pions, is also pronounced. This same dependency is also visible in some bins of figure 7, which depicts the beam-helicity asymmetry for negative pions as a function of z for different bins in x (row) and $P_{h \perp}$ (columns), however, overall limited statistical precision prevents further firm conclusions.

In summary, the here presented measurements are valuable results that serve the determination of parton distribution functions describing the distribution of quarks as a function of their longitudinal and transverse momenta inside a transversely polarized proton. Together with measurements from other experiments, they serve as input to the global analysis of these distributions. Also, the extraction of the subleading-twist beam-helicity asymmetry, sensitive to quark-gluon-quark correlations, contributes to cast light on the intricate quark-gluon-quark correlations inside the nucleon.

References

- [1] A. Bacchetta *et al.*, JHEP **0702** (2007) 093.

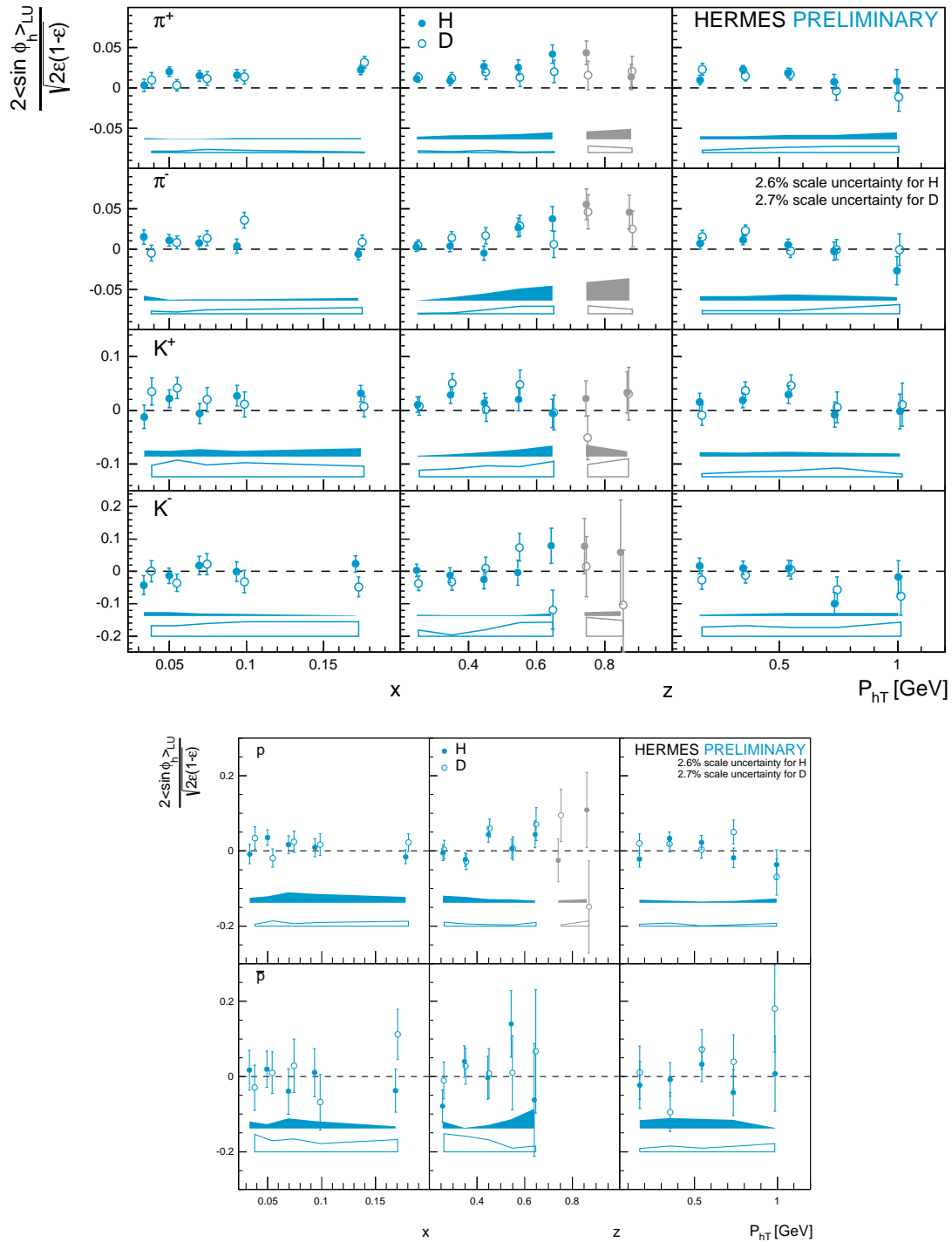


Figure 6: The beam-helicity amplitude for charged pions and kaons (top) and protons and antiprotons (bottom) as a function of x (left panel), z (middle panel) and $P_{h\perp}$ (right panel) for data collected on a hydrogen target (filled circles) and deuterium target (open circles). The error bars (bands) indicate the statistical (systematic) uncertainty. The data corresponding to the last two bins in z , depicted in grey, are not included in the projections as a function of x and $P_{h\perp}$.

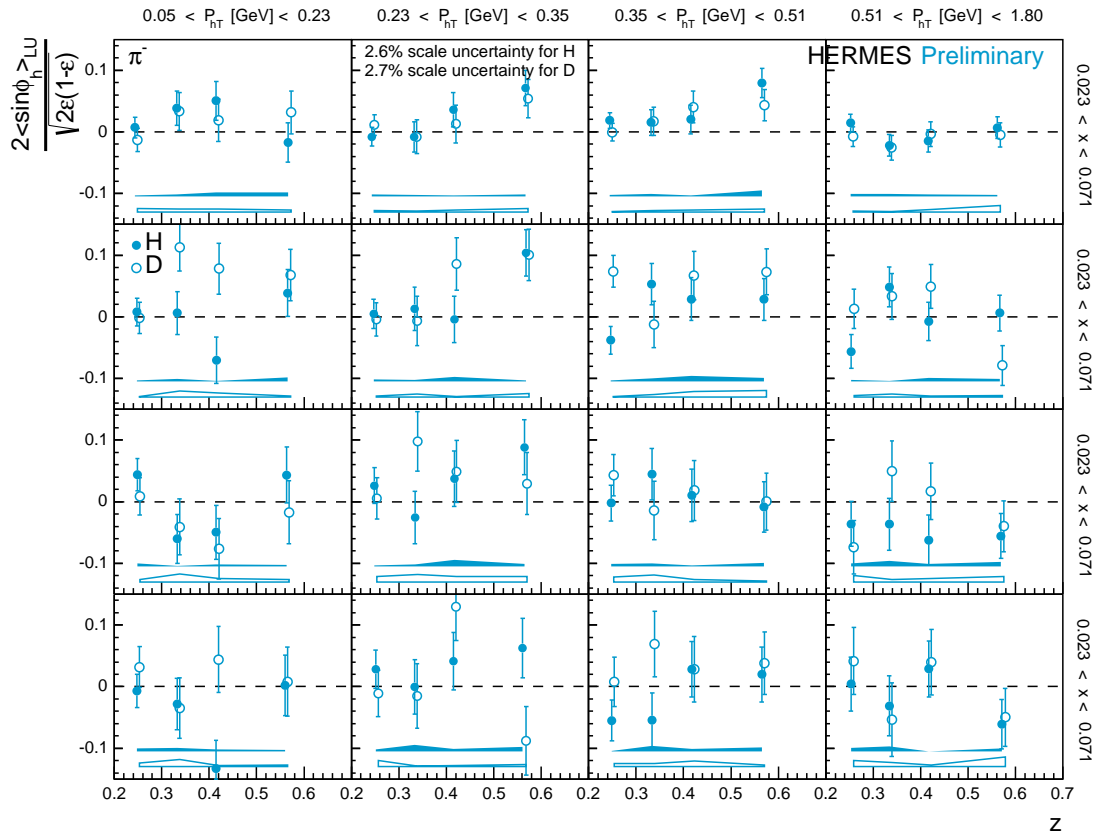


Figure 7: The beam-helicity amplitude for negatively charged pions as a function of z for different bins in x (rows) and $P_{h\perp}$ (columns) for data collected on a hydrogen target (filled circles) and deuterium target (open circles). The error bars (bands) indicate the statistical (systematic) uncertainty.

- [2] A. Airapetian *et al.*, Phys. Rev. Lett. **94** (2005) 012002.
- [3] A. Airapetian *et al.*, Phys. Rev. Lett. **103** (2009) 152002.
- [4] A. Airapetian *et al.*, Phys. Lett. B **693** (2010) 11-16.
- [5] L. L. Pappalardo, on behalf of the HERMES Collaboration, AIP Conf. Proc. **1441** (2012) 1-939.
- [6] A. Airapetian *et al.*, Phys. Lett. B **648** (2007) 164-170.